IL NUOVO CIMENTO Vol. 36 C, N. 4 Luglio-Agosto 2013
DOI 10.1393/ncc/i2013-11547-9

Communications: SIF Congress 2012

Photonic hydrophones based on coated fiber Bragg gratings

M. Pisco(*)

Optoelectronics Division, Engineering Department, University of Sannio
Corso Garibaldi 107, 82100 Benevento, Italy

ricevuto il 17 Febbraio 2013

Summary. — The development of underwater acoustic sensors with performances competitive with conventional piezoelectric hydrophones would overcome intrinsic limitations related to the piezoceramic technology. Optical fiber technology represents a valid platform to implement acoustic sensors for underwater scenarios. Here we report on recent numerical and experimental results obtained with photonic hydrophones based on fiber-Bragg-grating (FBG) with ring shaped coatings. Our numerical results fully characterize the opto-acoustic response of the optical hydrophone, and highlight the key role played by the coating in enhancing significantly its sensitivity by comparison with a standard uncoated configuration. Furthermore, the analysis reveals that the hydrophone sensitivity spectrum exhibits characteristic resonances, which strongly improve the sensitivity with respect to its background level. Our experimental results confirmed the expected resonant behavior of such devices and are in good agreement with the numerical predictions. Optical hydrophones based on coated FBG exhibited an excellent capability to detect acoustic waves in the acoustic frequency range, with extremely high sensitivities. By comparison with bare FBGs, sensitivity enhancements of up to three orders of magnitude were found, demonstrating the effectiveness of polymeric coatings in tailoring the acoustic response of FBG-based hydrophones.

PACS 42.81.Pa – Sensors, gyros.
PACS 42.79.Dj – Gratings.
PACS 43.30.+m – Underwater sound.
PACS 43.60.Vx – Acoustic sensing and acquisition.

1. – Introduction

Underwater acoustic sensors are widely used in civilian and military applications as SONAR devices. The best established technology relies on piezoceramic (lead zirconate titanate — PZT) hydrophones which convert an acoustic wave into an output voltage directly related to the wave amplitude by exploiting the piezoelectric effect.

(*) E-mail: pisco@unisannio.it

The performances of this class of sensors, in terms of acoustic detection capability, are remarkable, since they are able to sensing down to the deep-sea acoustic background.

Nevertheless, inherently to the technology, there are several limitations for in-field applications. Part of the electronics for the multiplexing and the related telemetry is immersed in water (and hence subjected to continuous harm and degradation) and is rather heavy and bulky because of the wiring. The scenario becomes even harsher when taking into account the water infiltrations which often occur during medium- and long-term explorations, with the consequent detrimental effects of performance degradation and malfunctioning.

The development of the underwater acoustic sensors with performances competitive with conventional piezoelectric hydrophones but based on a different technology such as photonics could circumvent the aforementioned limitations. In particular, fiber-optic sensors have the advantages of providing large dynamic range, high bandwidth, lightness, small size, wavelength multiplexing capability, immunity to electromagnetic interference, absence of electrical parts (especially important for underwater applications) [1].

Several sensing configurations have been proposed which rely on optical technology for acoustic detection in underwater scenarios.

A promising approach was proposed by Hill *et al.* [2], by using a distributed feedback fiber laser (DFB FL) as sensing element. The frequency of light produced by the DFB FL was extremely sensitive to acoustic perturbations. In [3], Foster *et al.* obtained a sensitivity of 100 nm/MPa by using a metal housing for the DFB FL sensor in order to enhance the hydrophone response. Even though DFB FL provides respectable sensitivities, and in-field demonstration of an FL hydrophone array has been also reported [4], sophisticated configurations are needed involving active doped fibers, pump laser, etc..

Recently Kilic *et al.* [5] have presented a micromachined fiber microphone consisting of a tiny Fabry-Pérot formed by a thin ($\sim$ 500 nm) photonic-crystal diaphragm placed at short distance from a mirror deposited at the tip of a single-mode fiber (SMF). The fabrication of photonic-crystal diaphragm onto the optical fiber tip, even if intriguing and paving the way for futuristic scenarios, it is obviously complex and it required sophisticated technologies able to create a pattern of holes through the dielectric layer.

Simpler approaches have been proposed based on the use of Fiber Bragg Gratings (FBGs) in standard optical fibers for acoustic detection.

Optical sensors based on FBG demonstrated to be suitable as underwater acoustic sensors by exploiting relatively cheap and well-established methodologies and technologies (*i.e.*, multiplexing strategies, interrogation units, etc.) already developed for various FBG communication and sensing applications.

A FBG, indeed, is constituted simply by a periodic modulation of the refractive index in the core of an optical fiber [6]. Such a periodic pattern, impressed in the optical fiber with well assessed and low-cost technologies [6], basically behaves spectrally as a narrow ($\sim$nanometers) reflective mirror at a specific wavelength, named Bragg wavelength. The Bragg wavelength is linearly related to the effective refractive index of the fundamental mode propagating in a single-mode optical fiber and to the grating period (pitch).

When sound pressure is applied to the FBG, the center wavelength is expected to vary in synchronization with the sound. This is true not only because the refractive index of the FBG is modulated by the pressure on the FBG due to the photoelasticity, but also because the physical length of the fiber and therefore the pitch of the grating is modulated by the external pressure on the fiber.

Unfortunately, in the case of uncoated FBGs, the mechanical deformation of the fiber due to the incident pressure is limited by the high Young's modulus (72 GPa [7]), leading

to a poor sensitivity.

An effective strategy to overcome this limitation was suggested by Hocker [8-10], by recognizing that low-elastic-modulus ring-shaped coatings may yield significant pressure sensitivities. Starting from this work, FBGs coated with materials characterized by Young's modulus lower than that of the fiber glass were proposed as promising hydrostatic pressure sensors [7].

Although the theoretical/numerical analysis carried out by Hocker [8-10] was limited to the hydrostatic case and cannot rigorously be extended to the acoustic case, experimental evidence of acoustic sensitivity optimization in the case of coated FBGs was recently demonstrated [11, 12].

Against this background, we carried out a systematic numerical analysis of the response of a coated FBG acting as an acoustic wave sensor. More specifically, we studied the complex opto-acousto-mechanical interaction among an incident acoustic wave traveling in water, the optical fiber surrounded by the ring-shaped coating, and the FBG inscribed in the fiber, via full-wave numerical simulations by means of a multiphysics software package based on the finite-element method (FEM). In order to provide a full characterization of the sensor performance, we also carried out a comprehensive parametric analysis of the hydrophone sensitivity, by varying the geometrical and mechanical properties of the coating [13, 14].

Finally, we performed an experimental characterization of coated FBG hydrophones. Specifically, we designed a set of FBG hydrophones with ring-shaped coatings characterized by different size and mechanical properties, in order to elucidate their impact on the acoustic response of the final device. These hydrophones have been fabricated and experimentally characterized within the frequency range 4–35 kHz by means of a suitably equipped tank [15]. Outcomes from the numerical and experimental analysis of the photonic hydrophones based on coated FBGs are also reported and discussed [15, 16].

2. – Numerical analysis

We present the study of the acousto-optic behavior of underwater-acoustic sensors constituted by FBGs coated by ring-shaped overlays. Via full-wave numerical simulations, we study the complex opto-acousto-mechanical interaction, schematically sketched in fig. 1a, among an incident acoustic wave traveling in water, the optical fiber surrounded by the ring-shaped coating, and the FBG inscribed the fiber, focusing on the frequency range 0.5–30 kHz of interest for SONAR applications.

In our simulations, performed by the Finite Element Method via the commercial software package COMSOL Multiphysics® [14], the underwater acoustic sensor under investigation is schematically represented by a 3D structure (fig. 1b) composed by an inner cylinder (the optical fiber), with height h and radius R_f, and an outer annular cylinder (the ring shaped coating), with same height h and coating radius R_C. From the acousto-mechanical viewpoint, no distinction is made between the core and the cladding of the fiber. The sphere of radius R_w in fig. 1b represents the water-filled acoustic domain surrounding the hydrophone.

The observable "sensitivity" (also referred to as responsivity [16]) can be defined as

$$S = \frac{\Delta\lambda}{\lambda_0 p_0} = \frac{1}{p_0}\left\{\varepsilon_z - \frac{n_{eff}^2}{2}\left[p_{11}\varepsilon_x + p_{12}\left(\varepsilon_z + \varepsilon_y\right)\right]\right\}, \tag{1}$$

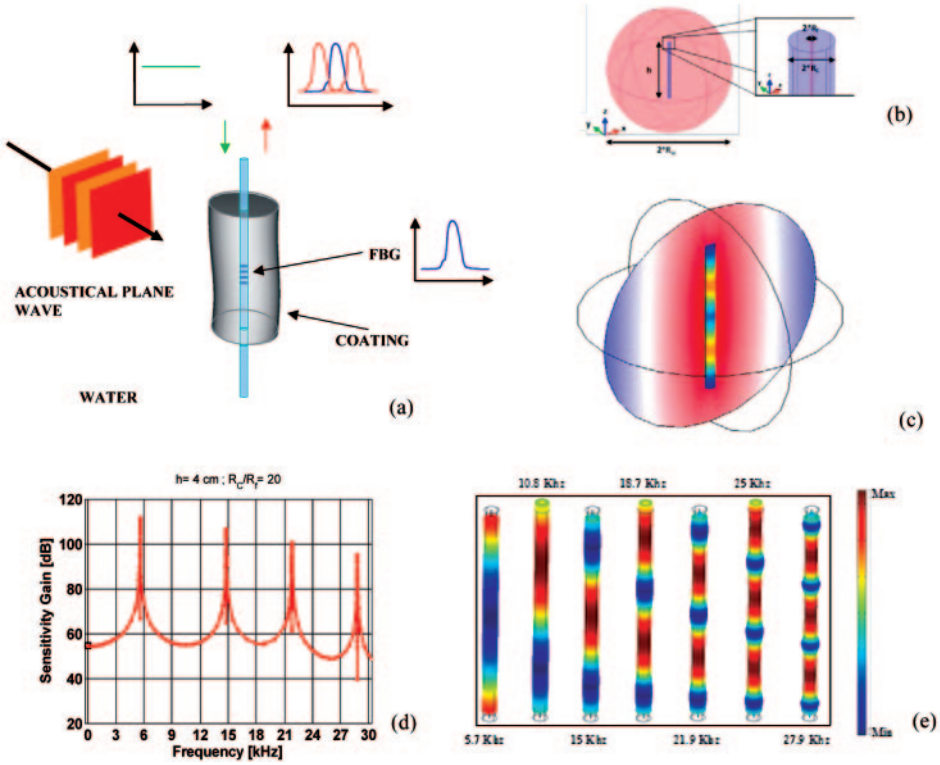

Fig. 1. – (a) Schematic description of the operational scenario for the underwater optical-fiber hydrophone. (b) 3-D geometry considered in the numerical simulations. (c) Pressure distribution in water and z-strain distribution on the cylinder surface at 20 kHz. (d) Sensitivity gain spectrum. (e) Deformed geometry and z-strain distribution (in color scale) of the resonant modes [14].

where $\Delta\lambda$ is the Bragg wavelength shift, λ_0 is the central wavelength of the FBG, p_0 is the acoustic-wave amplitude, $p_{11} = 0.121$ and $p_{12} = 0.265$ are the elasto-optic parameters, $n_{eff} = 1.465$ is the effective refractive index, and $\varepsilon_i (i = x, y, z)$ are the Cartesian strain components evaluated at the FBG location. Moreover, from the ratio between the calculated sensitivity and that pertaining to the bare (*i.e.*, without coating) fiber in the hydrostatic case (following [7]), a sensitivity gain may be defined as

$$\text{Sensitivity Gain} = 20 \log_{10} \left(\left| \frac{S}{S_{BARE}} \right| \right), \tag{2}$$

where $S_{BARE} = -2.76 \cdot 10^{-6}\,\text{MPa}^{-1}$ [12, 14].

In order to analyze the opto-acoustical response of our proposed sensor, we begin considering a specific configuration with fixed coating size and material properties, and investigate the interaction with an acoustic wave from the phenomenological viewpoint.

The configuration of interest features a ring-shaped coating with an outer radius $R_c = 1.25\,\text{mm}$ (*i.e.*, 20 times larger than the fiber radius) and a height $h = 4\,\text{cm}$. The elastic properties of the coating, are consistent with the nominal properties of a specific thermosetting polyurethane (Electrolube UR5041) [14], having a Young's modulus of

78 MPa, a Poisson's ratio of 0.3 and a density of 1180 kg/m^3. The structure is excited by an acoustic plane wave normally incident with respect to the cylinder axis.

As an illustration of the opto-acoustic response of the sensor to the impinging plane wave, fig. 1c shows the pressure distribution in water (on a slice) and the z-strain distribution on the cylinder surface, at 20 kHz (away from resonances). As evident in the figure, the cylindrical sensor responds to the impinging plane wave through a mechanical deformation, according to its elastic properties whereas the resulting strain at the FBG location determines a Bragg wavelength shift.

The sensitivity of this basic transduction principle is strongly enhanced at the resonant frequencies, as shown in fig. 1d. The hydrophone sensitivity spectrum, indeed, exhibits characteristic resonances (peaks in the sensitivity gain), which strongly improve the sensitivity with respect to its background (*i.e.*, away from resonances) level. All the observed resonances clearly resemble the Fano line-shape (in the strain and in the sensitivities curves) and may be accurately fitted with a Fano-type model. Recalling that Fano resonances stem from the interference between a discrete state with a continuum of states, we can infer that the resonances observed are attributable to the interaction between one of the vibration modes of the sensor and the impinging acoustic wave.

Via a three-dimensional modal analysis, we verify that the resonant features characterizing the hydrophone sensitivity are attributable to the excitation (by the normally-incident pressure plane wave) of longitudinal vibration modes (in fig. 1e) with even symmetry. From the phenomenological viewpoint, this observation somehow resembles the excitation of guided resonances in periodic or quasi-periodic photonic crystals [17-19]. In fact, more in general, we observed that only the longitudinal vibration modes of the composite structure that exhibit a symmetry matching that of the impinging pressure plane wave are excited.

In order to evaluate the sensor performance, we also carry out a comprehensive parametric analysis by varying the geometrical and mechanical properties of the coating, such as the coating height h, the coating radius R_C, Young's module E, Poisson's ratio ν, the density ρ', and the loss factor η. In all the simulations below, we assume the optical fiber radius equal to 62.5 μm, an optical fiber Young's modulus of 72 GPa, an optical fiber Poisson's ratio of 0.17, an optical fiber density of 2200 kg/m^3, a water density of 997 kg/m^3, a speed of sound in water of 1480 m/s.

The results from our comprehensive parametric studies are briefly summarized in fig. 2. They indicate that the coating height and radius may be effectively utilized in order to tune the resonant frequencies. Furthermore, larger coating radii may be beneficial in improving the low-frequency background sensitivity (but detrimental in the high-frequency region). In connection with the coating elastic properties, low values of Young's modulus, Poisson's ratio, and density are desirable for enhancing the sensitivity. Basically, decreasing Young's modulus and/or Poisson's ratio reduces the bulk modulus K of the ring-shaped coating (given by $K = E/[3(1-2\nu)]$, for homogeneous, isotropic, linear elastic materials) which, for a given acoustic pressure, yields in turn an increase of the coating compression, and hence an enhancement of the strain components acting on the FBG. Further insight may be gained by considering the *characteristic acoustic impedance* Z of the material composing the ring-shaped coating, defined as [14]

$$Z = \rho' c_C = \rho' \sqrt{\frac{K}{\rho'}} = \sqrt{\frac{\rho' E}{3(1-2\nu)}}, \tag{3}$$

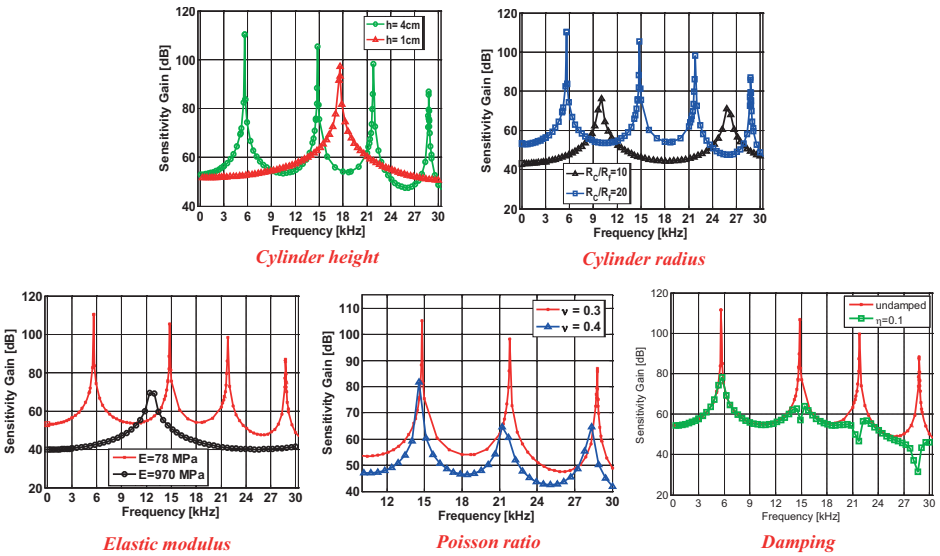

Fig. 2. – Sensitivity gain spectra of an hydrophone characterized by a ring-shaped coating with an outer radius $R_c = 1.25\,\text{mm}$ (*i.e.*, 20 times larger than the fiber radius), a height $h = 4\,\text{cm}$, a Young's modulus of 78 MPa, a Poisson's ratio of 0.3, a density of $1180\,\text{kg/m}^3$ and zero damping, by singly varying the cylindrical coating height, the cylindrical coating radius, Young's modulus E, coating Poisson's ratio ν and the damping (loss factor), respectively [14].

where c_C is the bulk speed of an elastic wave in a linearly elastic solid. It can readily be noticed that the sensitivity optimization criteria emerged from the parametric analysis are consistent with a *minimization* of the coating impedance. It is also worth noting that such minimization implies an increase of the impedance mismatch with the surrounding water, which is detrimental in terms of increased signal reflection, but is largely compensated by the increase of the strain energy endowed to the FBG.

Finally, it can be noted that the damping affects primarily the resonances (especially those at higher frequencies), yielding a strong sensitivity deterioration, while the baseline sensitivity gain turns out to be essentially unaffected. Since our model does not take into account the frequency-dependence of the coating elastic properties, the stronger deterioration effects observed at higher frequencies may be attributed to the corresponding longer acoustic paths in the coating. The effect of damping on the sensitivity must be carefully taken into account in the choice of the coating material, since a low Young's modulus (useful to increase the sensitivity) is often competing with a low damping, because "soft" materials typically exhibit high damping.

3. – Experimental results

Based on our previous numerical results, we designed a suitable set of FBG hydrophones, taking into account three main objectives [16]:

i) to experimentally demonstrate the resonant behavior in the sensitivity (insofar observed only numerically);

ii) to analyze the influence of the cylindrical coating features on such resonant behavior;

iii) to fabricate several hydrophones characterized by different spectral responses and, more specifically, with resonances at frequencies lower and higher than 15 kHz.

In particular, coatings based on materials with low Young's modulus were designed so as to yield resonances occurring in the low frequency range, whereas materials with high Young's modulus were exploited in the high-frequency range.

To this aim, the selected coating materials were characterized by relatively "low" and "high" Young's modulus: Damival® E 13650 and Araldite® DBF.

The former is a polyurethane resin, commonly used to overcoat piezoceramic acoustic transducers without degrading their performance, which exhibits a Young's modulus on the order of few hundreds MPa, and a low acoustic impedance to enhance the coating elastic response to the impinging wave. The latter is a low-viscosity epoxy resin containing a plasticizer, typically used as strong adhesive, and characterized by a Young's modulus of 2.9 GPa. In spite of the higher Young's modulus of the Araldite® DBF coating, it is also characterized by a significantly lower loss factors, useful to avoid detrimental effects on the resonant behavior at high frequencies.

Overall, we numerically designed and experimentally analyzed three sensors with the following characteristics:

1. Damival sensor, with coating diameter and length of 5 mm and 40 mm, respectively;
2. Araldite sensor, with coating diameter and length of 5 mm and 38 mm, respectively;
3. Damival sensor, with coating diameter and length of 10 mm and 40 mm, respectively.

The fabrication of the designed FBG hydrophones was carried out by means of a set of appropriate holders [16]. In particular, for Damival-based sensors, a modular holder was designed so as to obtain a cylindrical coating on the fiber grating with desired size (in terms of sensor diameter and length). Moreover, in order to reduce mechanical stresses on the lead-in and lead-out fiber cables, the holder was designed so as to leave two conical regions (of the same material, and ~ 10 mm long) on both ends of the cylindrical region. Such modular holder enabled for the realization of Damival sensors with diameter of 5 mm and 10 mm (henceforth, simply referred to as D-5 and D-10, respectively), while the length (selectable with steps of 10 mm) was fixed at 30 mm for both sensors.

Conversely, in view of its low viscosity and high adhesive characteristics, a different configuration was implemented for the Araldite-based sensor. In this case, the holder (with diameter and length of 5.0 mm and 38 mm, respectively) is non-modular in order to avoid the resin insertion between the modules, and there are no conical regions at the ends. A picture of sensors D-5 sand A-5 is shown in fig. 3.

Field trials were carried out in an instrumented tank at the Whitehead Alenia Sistemi Subacquei Laboratory (Naples, Italy). Details on the setup for the experimental characterization can be found elsewhere [15, 16]. Basically, a train of sine-wave pulses with duration 0.5 ms at increasing frequencies in the range 4–30 kHz (with step of 1 kHz) is generated by an acoustic source immersed in the water tank, while reference data have been retrieved using a reference PZT hydrophone. The FBG hydrophones were vertically positioned and kept by means of a few gram weight. Consequently, the sound pressure was perpendicular to the fiber longitudinal axis. For each frequency, the resulting time responses of the coated FBGs sensors to the acoustic excitation were measured via a tunable laser locked to work at the edge of the FBG spectra. From the time responses

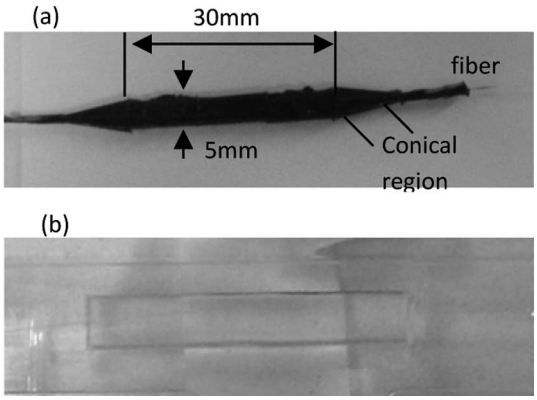

Fig. 3. – Pictures of FBG hydrophones (a) D-5 and (b) A-5 [16].

(corresponding to the acoustical sine-wave pulses), the amplitudes of optical sensor responses have been obtained through FFT analysis and used to reconstruct the sensitivity curve *vs.* frequency.

The obtained experimental sensitivity gains are reported in fig. 4(a-c). In the same plots the corresponding numerical predictions are also shown for comparison. A good agreement between the experimental data and the numerically predicted sensitivity gains can be clearly appreciated. It is worth to note that the elastic properties of the polymeric coatings used to numerically reconstruct the experimental data are consistent with those found in literature for both class of materials [14]: polyurethane resins for Damival® E 13650 ($E = 200\,\mathrm{MPa}$, $\nu = 0.4$, $\eta = 0.1$, $\rho' = 1180\,\mathrm{kg/m^3}$) and Araldite® based resins for Araldite® DBF ($E = 2.9\,\mathrm{GPa}$, $\nu = 0.345$, $\eta = 2 \cdot 10^{-2}$, $\rho' = 1100\,\mathrm{kg/m^3}$).

The comparison primarily confirms the resonant behavior of the underwater acoustic sensor outlined by the numerical analysis, which in turn demonstrates to be able to supply physical insight in the sensor operation and at the same time to offer acceptable prediction capabilities both in terms of resonant frequencies and sensitivity values.

The disagreements between experimental and numerical data (particularly evident with the Araldite® coating) can be attributed to second order effects (physical imperfections, acoustically induced particle fluid motion, ...), which have not been taken into account in the simulations, but that are not able to dominate the basic transduction mechanism.

A major difference between the experimental and numerical data can be found in the shape of the sensitivity gain peaks. Differently from the experimental observations, the numerical predicted Fano line shape in the sensitivity would imply a zero crossing for the sensitivity and thus a narrow dip in the sensitivity gain for each resonance (actually the dip is well appreciable in the numerical plots only when a fine frequency sampling is employed).

From the experimental viewpoint, these narrow spectral features cannot be appreciated due to the finite duration of a single acoustic tone (0.5 ms) limiting the spectral resolution of the experimental characterization (in turn experimentally the pulse duration is limited in order to avoid the superposition of the direct wave with the reflected ones in the tank). To better explain the effect of the limited spectral resolution on the numerical predictions, in fig. 4(a-c) we show (with the trace "elaborated") the numerical

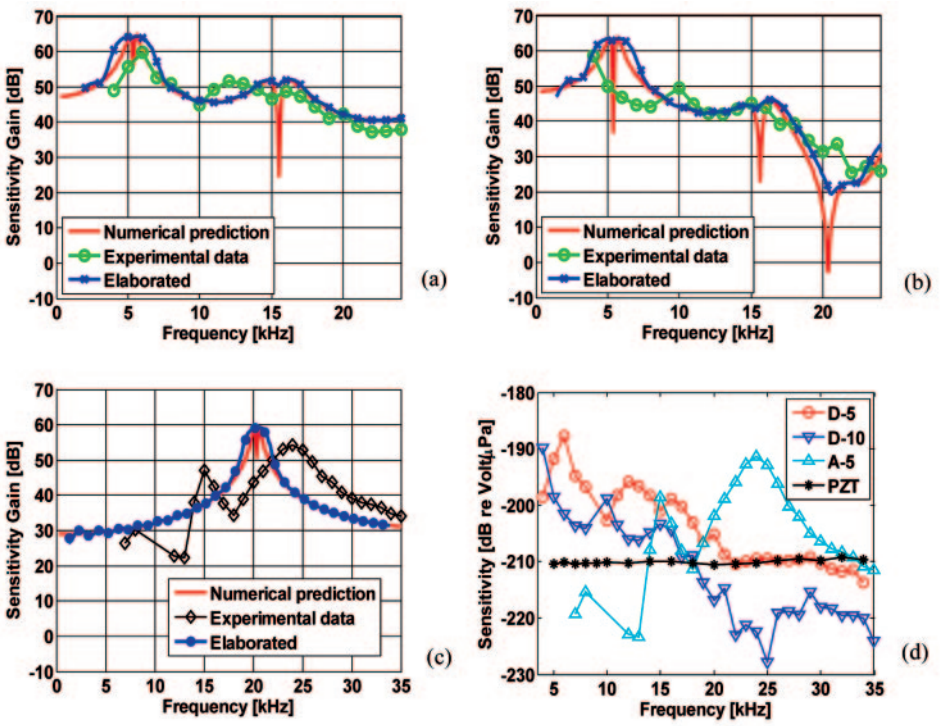

Fig. 4. – Numerical and experimental sensitivity gain of a coated FBG respect to bare fiber *vs.* frequency (a) for the D-5 sensor, (b) for the D-10 sensor and (c) for the A-5 sensor. Elaborated data take into account the smoothing effect of the finite input signal duration. (d) Experimental sensitivity spectra of the three fabricated FBG hydrophones in terms of dB re V/μPa. The sensitivity of the PZT reference hydrophone is also shown [16].

sensitivity gain accounting for the finite duration of the acoustic pulse. It is evident in fig. 4 that the finite time extent of the sine wave pulses smoothes the sharp spectral features by strongly deemphasizing the presence of the narrow dips and justifying the difference between numerical and experimental data in the peaks shapes when this effect is not taken into account.

In order to compare the spectral behavior of the optical hydrophones with that of the reference PZT, the sensitivities of the four devices, calculated as dB re V/μPa, are shown in fig. 4d.

It can be seen that the sensitivities of the optical devices based on Damival coatings are significantly higher than that of the reference PZT within the range 4–21 kHz.

On the contrary, the sensitivity of the Araldite-based device results significantly higher than the PZT reference hydrophone for higher frequencies due to the sensor resonance at ~ 24 kHz, with sensitivity ~ -191.3 dB re V/μPa (by comparison with -209 dB re V/μPa for the reference PZT).

From the above results, and taking into account the noise floor of the set-up utilized (currently not optimized), a minimum detectable acoustic signal of about 10 mPa/Hz$^{1/2}$ can be obtained around the resonances of both Damival and Araldite hydrophones.

Although the experimentally demonstrated sensitivities are comparable with those of PZT detectors, the achieved limit of detection is higher (worse) than that required for

passive acoustic detection, and an improvement of at least two orders of magnitude is necessary for practical implementations.

Nevertheless, on the basis of the results presented, the coated FBGs could efficiently work in realistic applications dealing with active acoustic detection where the resonant behavior could be efficiently adopted in combination with suitable synchronous demodulation schemes.

Moreover, our results demonstrated a significant improvement up to three orders of magnitude with respect to the state of the art of passive FBG sensors for underwater acoustic sensing. Furthermore, the present investigation provides a clear understanding of the physical mechanism at the basis of the observed resonant behavior, setting the stage to suitable performance tailoring for specific applications.

Preliminary results on sensors array and an offshore testing (reported elsewhere [16]), carried out in the Bacoli bay (Naples, Italy), provided further confirmation of the great potential of the proposed technology for practical acoustic monitoring applications.

4. – Conclusions

In summary, we have reported the first evidence of the resonant behavior of an underwater acoustic sensor constituted by an FBG coated by a ring-shaped material. We have carried out a full 3D numerical analysis of this acoustic sensor in the frequency range 0.5–30 kHz, thereby extending previous studies on coated FBGs limited to approximate hydrostatic modeling.

Our numerical results fully characterize the opto-acoustic response of the optical hydrophone, and indicate that the coating may significantly enhance the sensitivity over the whole investigated frequency range, by comparison with an uncoated FBG. The excitation of characteristic resonances (at frequencies related to the physical and geometrical parameters) of the cylindrical coating further improves the sensor performance.

Our full-wave numerical analysis, besides providing a physical insight in the interaction between the impinging acoustic wave and the sensor, also gives useful hints and guidelines for the design and performance optimization towards specific applications. For instance, the resonant behavior can be better exploited in active acoustic sensing applications whereas the sensor behavior in a frequency range away from the resonances seems better suited for passive acoustic sensing.

Additionally, we have reported the results of a performance analysis of FBG hydrophones for underwater sound pressure detection, carried out within the frequency range 4–35 kHz.

Our experimental results confirmed the expected resonant behavior of such devices and are in quite good agreement with the numerical predictions.

Optical hydrophones based on coated FBG exhibited an excellent capability to detect acoustic waves in the investigated frequency range, with extremely high sensitivities.

* * *

I am very grateful to the conference organizers for the invitation to make this contribution. The described research activities have been possible thank to Massimo Moccia, Marco Consales, Agostino Iadicicco, Antonello Cutolo, Vincenzo Galdi, and Andrea Cusano and thank to the support of the Whitehead Sistemi Subacquei (WASS) for the availability of the instrumented water tank and S. Passaro, E. Marsella, S. Mazzola for their support in the offshore tests.

REFERENCES

[1] Wild G. and Hinckley S., *IEEE Sensors J.*, **8** (2008) 1184.
[2] Hill D. J. and Nash P. J., *Proc. SPIE*, **4185** (2000) 33.
[3] Fosters S., Tikhomirova A., Milnesa M., van Velzena J. and Hardyb G., *Proc. SPIE*, **5855** (2005) 627.
[4] Goodman S., Foster S., Van Velzen J. and Mendis H., *Proc. SPIE*, **7503** (2009) 75034L1.
[5] Kilic O., Digonnet M. J. F., Kino G. S. and Solgaard O., *Meas. Sci. Technol.*, **18** (2007) .
[6] Erdogan T., *J. Lightwave Technol.*, **15** (1997) 1277.
[7] Hill D. J. and Cranch G. A., *Electron. Lett.*, **35** (1999) 1268.
[8] Hocker G. B., *Appl. Opt.*, **18** (1979) 3679.
[9] Hocker G. B., *Opt. Lett.*, **4** (1979) 320.
[10] Hocker G. B., *Appl. Opt.*, **18** (1979) 1445.
[11] Cusano A., D'Addio S., Cutolo A., Campopiano S., Balbi M., Balzarini S. and Giordano M., *Sens. Trans. J.*, **82** (2007) 1450.
[12] Cusano A., Pisco M., Parente G., Lanza G., Laudati A., Giordano M., Campopiano S. and Cutolo A., *Europe Security and Defence 2009*, in *Proc. SPIE*, **7482** (2009) 74820I.
[13] Moccia M., Pisco M., Cutolo A., Galdi V. and Cusano A., *Proc. SPIE*, **7753** (2011) 775384.
[14] Moccia M., Pisco M., Cutolo A., Galdi V., Bevilacqua P. and Cusano A., *Opt. Express*, **19** (2011) 18842.
[15] Moccia M., Consales M., Iadicicco A., Pisco M., Cutolo A. and Cusano A., *Proc. SPIE*, **7753** (2011) 775383.
[16] Moccia M., Consales M., Iadicicco A., Pisco M., Cutolo A., Galdi V. and Cusano A., *J. Lightwave Technol.*, **30** (2012) 2472.
[17] Sakoda K., *Phys. Rev. B*, **52** (1995) 7982.
[18] Ricciardi A., Gallina I., Campopiano S., Castaldi G., Pisco M., Galdi V. and Cusano A., *Opt. Express*, **17** (2009) 6335.
[19] Gallina I., Pisco M., Ricciardi A., Campopiano S., Castaldi G., Cusano A. and Galdi V., *Opt. Express*, **17** (2009) 19586.